Hadron Calorimetry at the LHC

J. Proudfoot
Argonne National Laboratory, Argonne, IL 60439, USA

The hadronic calorimeter may not be the most glamorous detector system in LHC experiments, especially when compared to its cousin the electromagnetic calorimeter. Nonetheless, much of the LHC physics program would be inaccessible without. In this lecture, I discuss some of the physics requirements and the detector technology used in hadron calorimeters in ATLAS and CMS, the physics of hadron calorimeters in general as well as the techniques used to maximize the performance of these detector systems.

1. JETS CALORIMETERS AND ALL THAT

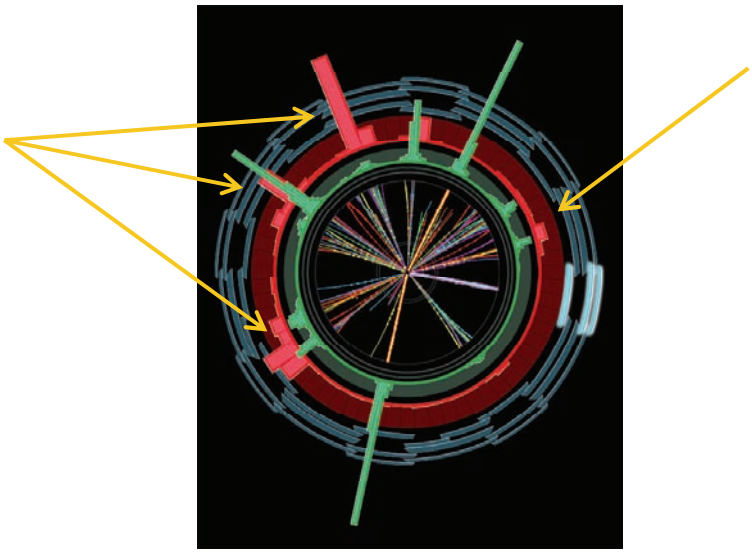

Figure 1, a cartoon (from simulation) showing the transverse view of an event at the LHC. Some of the jets in the event are indicated by the arrows.

Hadron Calorimeters are ***essential*** to measure jets and jets are ***essential*** for much of the LHC physics program. The jets themselves are collections of energy detected in a limited region of pseudo-rapidity and angle as expected from the fragmentation of quarks and gluons into hadrons. A cartoon showing a simulated event containing jets (and leptons) is shown in Figure 1. It shows all the basic characteristics of jets when viewed in the transverse plane – i.e. along the beam axis so that the boost in the event is not a factor. In this lecture I will first address issues associated with the physics measurements to be made. From this point I will present the fundamentals of a hadronic sampling calorimeter drawing from the specific example of one based on plastic scintillator as the sensitive medium. This leads into a discussion on the characteristic of the hadronic cascade and techniques by which the intrinsic performance of a calorimeter may be improved. Finally, I will conclude with a section presenting the challenge at the LHC, where one must optimize the reconstruction of the energy of ensembles of particles – QCD jets.

The list of physics processes for which jet measurement is required includes:

- The top mass measurement using the Top decay to Wb-bar in which the W decays to two quark jets. It is sensitive to the Higgs mass through loop corrections and as such provides either confirmation of Standard Physics or a glimpse of physics beyond the Standard Model. For this measurement the precision with which the jet energies are measured is of fundamental importance.
- QCD Production of Z and W bosons in association with 1, 2, 3, or more jets. For this study, it is essential to understand the jet energy profile to better discriminate 2 jets from a single larger jet as well as, to a lesser extent, the jet energy scale.
- Searches for SUSY include the observation of a high multiplicity of jets as one element in the signature. The precision with which jet transverse energy (E_t) is measured is a central factor in the measurement of missing transverse energy, which is a key signature for this physics.
- "Simple" jet kinematics, such as the jet E_t spectrum or Dijet mass spectrum provide windows into the highest energy scales at the LHC and form the basis for model independent searches for physics such as quark compositeness. Again for these studies the limiting experimental characteristic is the jet energy scale.
- Weak Boson Fusion production of the Higgs boson, which may indeed be the discovery channel. In this process, jets must be detected and well measured in the forward region of the detector and vetoed in the central region of the detector.

To perform these physics studies, we must understand the precision with which we can perform the following types of measurements:

- Count jets
- Measure jet energies and angles
- Use jets to estimate Standard Model backgrounds to new physics
- Veto events with jets in part of the detector acceptance
- Measure missing transverse energy, whether collected into jets or not

To meet these requirements one must have a calorimeter with lateral segmentation in order to measure jet angles and to separate jets. The calorimeter must be hermetic (i.e. have as complete coverage as possible) to measure all energy emitted from the interaction point and thereby infer missing transverse energy. If the calorimeter has a different response to electrons and hadrons, then longitudinal and lateral segmentation is necessary to allow for "software compensation". Finally, these measurements must be made over the maximum possible kinematic acceptance and as a result, calorimeters can be enormous. The ATLAS calorimeter has a diameter of about 8500cm, and a total length of about 12m. It is shown in Figure 2, where we can see that even this device is dwarfed by the ATLAS barrel toroid coils (the people are of course normal size.)

The characteristic, which differentiates between the required performance of calorimeters for LHC physics and past calorimeters, is ***precision***. The measurement of the top mass sets a representative scale. With 680pb-1, the CDF experiment recently measured the top mass with a precision of 2.8 GeV/c^2, in which the contribution to the systematic uncertainty coming from the jet energy scale is a mere 1.8 GeV/c^2. This uncertainty is reducing steadily as CDF and D0

accumulate more data, and with combined fits to the Tevatron results [1]. To achieve such precision in a hadronic system presents a considerable challenge to hadron calorimetry, and in fact the ATLAS goal is to measure the top mass with an uncertainty less than 1.3GeV (dominated by the jet energy scale systematic uncertainty [2].)

Figure 2, the ATLAS barrel calorimeter position inside the toroid magnets on the interaction point.

In this lecture I will address aspects of hadron calorimetry, which pertain to the operational reconstruction of jet kinematics. As the goal is to describe hadron calorimetry at the LHC, I will limit my discussion to sampling calorimeters of the type used in ATLAS and CMS and furthermore will illustrate most of their characteristics using the technology with which I have worked over the last 20 years – namely scintillator sampling calorimeter with wavelength shifting fiber readout, and which is used in the central hadronic calorimeters of both CMS and ATLAS. Of course there are other calorimeter technologies used in both CMS (crystal calorimeter) and ATLAS (liquid argon ionization calorimeter). Descriptions of these can be obtained from the web sites of ATLAS and CMS [3]. I will not address active compensation as realized in the ZEUS calorimeter using uranium plates as the absorber medium, nor will I discuss the physics of total absorption calorimeters as these are typically only of use for the measurement of electromagnetic showers. Finally, this is a lecture whose principal focus is detector technology and as a result I will not discuss the step which is required to connect the observed energy in the detector to the underlying parton energy - this would require an entire series of lectures.

2. HADRONIC CALORIMETER TECHNOLOGY

As is suggested by the name, a calorimeter measures energy. This is simply the total ionization energy, dE/dx deposited in an absorber by the cascade of particles produced when a high energy particle impinges on it (Figure 3.) A sampling calorimeter is then a calorimeter, which samples a fraction of the total energy deposited and we infer the total

energy of the incoming particle(s) from the ionization deposited in the sampling layers- usually by converting it to an electrical signal and digitizing it.

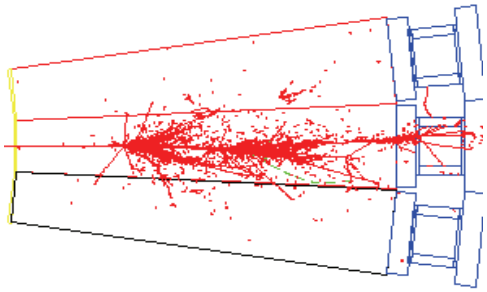

Figure 3, cartoon of the particle cascade resulting from the interaction of a high energy particle with the absorber of the ATLAS tile calorimeter.

There are many advantages to the use of calorimeters in particle physics:

- They measure neutrals as well as charged hadrons and photons
- Their resolution improves with energy
- They can cover a large fraction of the acceptance and therefore measure essentially all of the energy emitted in the physics interaction of interest
- They can provide a fast trigger

Unfortunately, they also have some disadvantages:

- They are typically big and therefore cost is a serious concern
- As an important aspect of their performance, they typically have a non-linear response and in particular a different response to electromagnetic and hadronic energy.

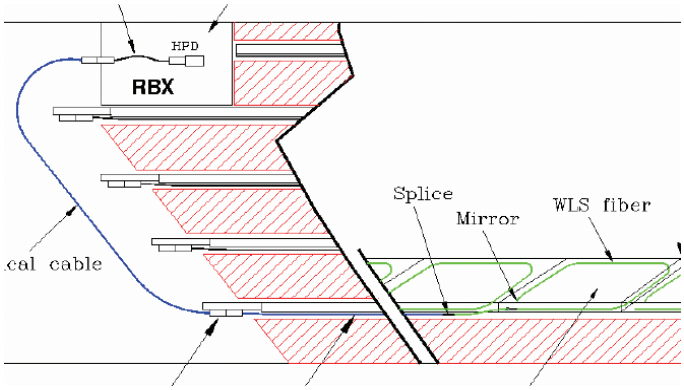

Figure 4, CMS hadronic calorimeter sampling geometry (schematic). Wavelength shifter fibers imbedded in the scintillator tiles couple the scintillation light to the HPD photo-detectors.

As stated in our requirements above, the function of a calorimeter is to measure ionization using a read out system, which allows sufficient segmentation to measure the kinematic properties of jets. In the central region the hadronic

calorimeters of ATLAS and CMS use plastic scintillator with wavelength-shifting fiber readout to perform this measurement. The basic concept is shown in Figure 4 (based on the CMS implementation) where each scintillator tile is read out by a separate fiber and the fibers then routed to the photo-detectors.

The physical segmentation of the scintillator tiles themselves, in conjunction with the fiber routing, is used to provide readout segmentation along the beam direction and in depth within the calorimeter. Segmentation in azimuth is achieved by constructing the full calorimeter from a number of modules each subtending a small angular range. The segmentation in pseudo-rapidity is particularly clear in the case of CMS, as is seen in Figure 5.

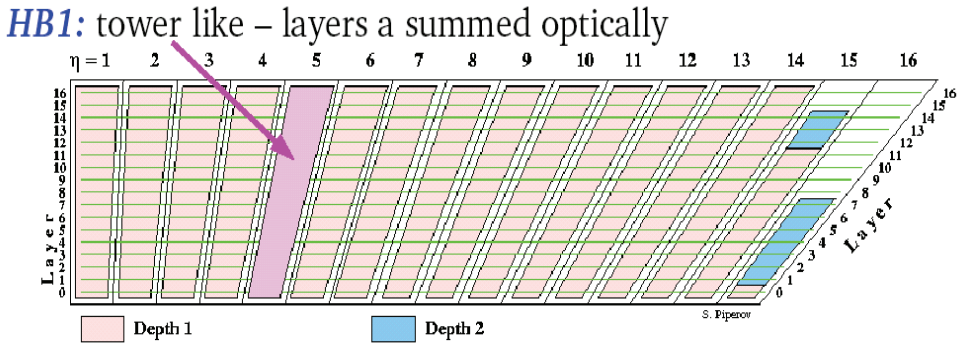

Figure 5, CMS projective geometry in pseudo-rapidity.

Plastic scintillator detects the passage of charged particles by the conversion of ionization energy to optical wavelength light. An excellent overview of scintillator properties, and in particular a discussion of saturation of the light output for highly ionizing particles can be found in [4] and I give only a brief description in this lecture. Charged particles traversing the scintillator tiles deposit ionization in optical quality plastic, which is doped with a primary fluor to convert the primary ionization to UV light. A second fluor in the plastic absorbs this radiation and emits light at a longer wavelength (typically in the blue) to allow this light to propagate to the edge of the scintillator with reasonably low loss of intensity due to attenuation. This scintillation light is absorbed by a third fluor in the wavelength shifting fiber, which is either imbedded in the scintillator or views its edge. This fluor then emits light at an even longer wavelength (typically green), which propagates by total internal reflection along the fiber to a photon detector, where it is converted to an electrical signal for digitization. In the case of CMS this photon detector is an Avalanche Photodiode, for ATLAS it is a conventional photo-multiplier tube. The final calibration of the observed signal cannot in general be derived from first principals but must be determined using the response of the calorimeter to high energy particle beams. A calibration system, such as can be realized using radio-active sources may then be used to maintain this basic calibration during detector operation. As we will see below, even in the most ideal case, more refined corrections are required to account for fluctuations in the observed response and non-linearity as a function of particle energy. These corrections must be obtained using a Monte Carlo simulation, which itself must be tuned to experimental data.

3. PERFORMANCE AND (COST) OPTIMIZATION

Energy deposition in the calorimeter is statistical and depends on the number of particles contributing to the cascade. This may be considered in terms of a critical energy, which in the case of a hadronic cascade can be taken as the energy

required for pion multiplication. Above this energy the number of particles in the shower continues to increase, whilst once all particles have energies below the critical energy then the shower dies off as they lose energy through ionization. In this model, the number of particles in the shower can be estimated as $N_{shower} \sim E_{particle}/E_{critical}$, with each particle contributing the same equivalent energy. The statistical nature of the process therefore results in the resolution $\sigma_E \sim 1/\sqrt{N_{shower}}$ and therefore the well known form for the energy resolution of $\sigma_E \sim 1/\sqrt{E_{particle}}$

The basic period of a sampling calorimeter is shown in Figure 6, where we see layers of absorber interspersed with layers of detector medium (scintillator in the case of ATLAS and CMS central hadron calorimeters.) The basic performance of such a calorimeter depends on two well-known factors [5]:

- Sampling fraction
- Sampling Frequency

The sampling fraction is defined as the fraction of ionization energy deposited in the active medium for minimally ionizing particles. Under the approximation that the total ionization is uniformly deposited, then it is linearly proportional to the ionization measured in the scintillator. In practice this approximation is not valid and even in the case of a device with linear charge response, such as a liquid argon ionization calorimeter, the primary calibration must be obtained from a combination of Monte Carlo simulation and testbeam data.

The resolution of the calorimeter is a function of the frequency with which the shower is sampled. This term, which scales as $1/\sqrt{}$(absorber plate thickness), is easy to visualize by simply comparing two configurations:

- A single absorber layer of total thickness $T_{abs}=T_a$ with a single ionization measurement layer.
- A total of N absorber layers of thickness $T_{abs}=T_a/N$ uniformly interspersed with N ionization measurement layers

Both configurations have the same sampling fraction but the second has an improved stochastic response, which is proportional to $\sqrt{T_{abs}}$, where the thickness is expressing in terms for radiation lengths for electromagnetic showers and interaction lengths for hadronic showers [5].

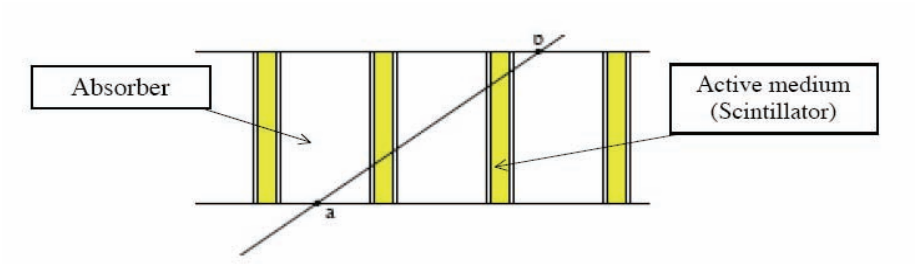

Figure 6, cartoon showing a sampling calorimeter with a particle traversing it.

The uniformity with which the ionization signal is measured in a given measurement layer also contributes to the resolution of a sampling calorimeter. One example of typical non-uniformity in light collection for scintillator-based calorimeters is shown in Figure 7, which shows the light signal collection as a function of the position at which the ionization energy is deposited.

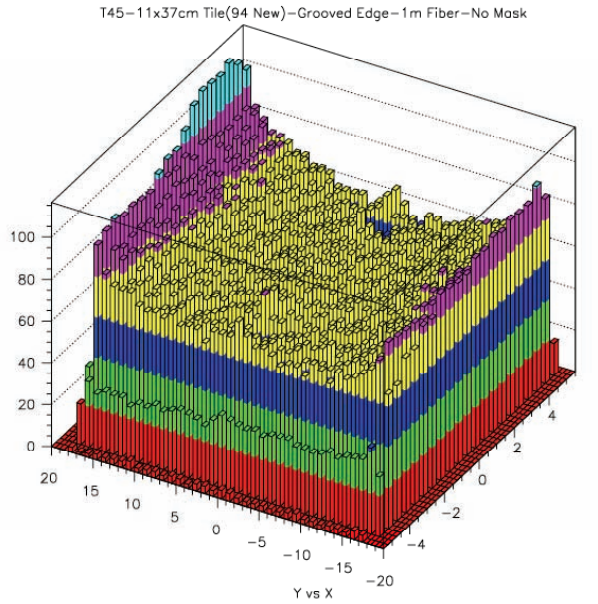

Figure 7, light collection efficiency across the surface of an (unmasked) tile, such as is used in the ATLAS Hadronic Tile Calorimeter. The scintillation light is read out using fibers which are coupled to the edges of the tile.

There are many other similar characteristics, which contribute to the resolution of a sampling calorimeter, including fiber coupling, absorber thickness uniformity, dead material between sampling layers (such as cryostat vessels and coils), light detection efficiency (such as coming from finite photo-statistics) and readout noise. These must be modeled (generally using a Monte Carlo simulation) and specifications developed for each characteristic of the detector design. If the basic non-uniformity does not meet specification, as is generally the case for light collection uniformity across the face of a scintillator tile, then correction techniques must be developed and incorporated into it (in this case a patterned reflective wrapper.) Some of the detector characteristics may also affect the intrinsic linearity of the calorimeter – an obvious example being non-linearity in the readout electronics. Finally, the calorimeter must be sufficiently deep to fully contain the showers of interest (i.e. at the highest energies.) For LHC energies, this is of order 10 interaction lengths.

CMS and ATLAS have arrived at quite different design goals and hadronic calorimeter optimizations:

ATLAS

- A design resolution, $\sigma_E/E \sim 50\%/\sqrt{E} + 3.0\%$
- Absorber plates of hadron calorimeter run normal to the beam line, fine sampling
- Accordion calorimeter for measurement of photons and electrons
- Cryostat and coil (containing ~0.4λ) is between the electromagnetic calorimeter and the first depth of the hadronic calorimeter

CMS

- A design resolution, $\sigma_E/E \sim 100\%/\sqrt{E} + 4.5\%$
- Cu absorber, coarse sampling
- A coarse sampling tail catcher outside the solenoid is used to give the necessary total depth

	t_{em}	t_{had}
ATLAS, Tilecal (Fe)	1.0	0.11
CMS HCAL (Cu)	3.5	0.33

Table 1, the absorber plate thickness, in terms of radiation length (t_{em}) and hadronic interaction length (t_{had}), used in the ATLAS and CMS central barrel calorimeters.

The different optimizations are quite striking as shown in Table 1. In particular, it is worth noting that the sampling thickness of the CMS hadronic calorimeter is 3.5 radiation lengths, which will result in a significant suppression in its response to the electromagnetic component of the hadronic cascade. Only time will tell if the design goals and physical realization of these detectors will fulfill the needs of the LHC experimental program.

4. HADRONIC SHOWERS

In Section 3 above, I introduced the 'mechanical" characteristics of sampling calorimeters as they pertain to their performance and the guiding principals which relate the measured ionization to the energy of the incident particle. According to this simplified model of track length, the ionization is linearly proportional to the energy of the incident particle. This is only very approximately true:

- scintillation light is not proportional to the deposited ionization – an effect termed "saturation" occurs and can be described by the well known formula of Birks [4],which provides an empirical description of the scintillation light output as a function of particle momentum and species
- there is an intrinsic difference in response of calorimeters to hadronic and electromagnetic showers ($e/h \neq 1$)
- binding energy losses contribute to a reduction in the observed ionization and their fluctuations contribute significantly to the degradation in resolution of a hadronic calorimeter

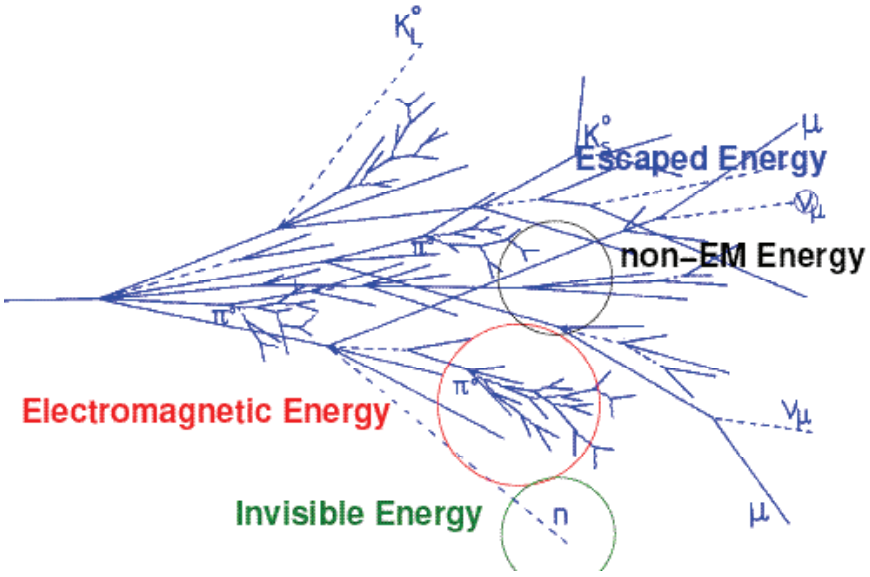

Figure 7, cartoon depicting the hadronic cascade initiated by a single charged hadron impacting an absorber.

We now turn to the physics of hadronic showers as this physics is central to the Monte Carlo codes used to simulate the calorimeter response and thereby determine corrections for effects such as those above, to optimize calorimeter resolution and linearity. A pictorial representation of a hadronic cascade is shown in Figure 7. The key observations are [6]:

- EM energy is ~50%
- Visible non-EM energy (dE/dx) ~ 25%
- Invisible non-EM energy (binding energy, nuclear breakup) ~ 25%
- Escaped energy (neutrinos) ~ 1%

The general characteristics of hadronic cascades were first measured some 30 years ago [7]:

- The early part of the shower has a dense core whose radial extent is consistent with coming from the deposition of electromagnetic energy
- The shower width increases approximately linearly with (depth × density)
- The late part of the shower is broad and is associated with the deposition of hadronic energy
- The contribution from the electromagnetic energy diminishes with shower depth

Detailed studies of the hadronic shower shapes were conducted during beam studies of the prototype Tile Calorimeter for ATLAS [8]. By scanning the beam across boundaries in calorimeter cells, the transverse size of the shower from high energy pions was measured at four depths in the calorimeter. The resulting shower shapes were fitted to a sum of 3 exponentials:

$$f(z) = E_0/2B \sum_{i=1}^{3} a_i e^{-|z|\lambda_i}$$

The fit yielded;

$\langle\lambda_1\rangle$ = 23mm
$\langle\lambda_2\rangle$ = 58mm
$\langle\lambda_3\rangle$ = 250mm

The distance scales are such that the first component is naturally attributed to electromagnetic energy deposition, whereas the second and third components are attributed to non-electromagnetic (hadronic) energy deposition. The amplitude of these three components as a function of depth in the shower is shown in figure 9a, which confirms the earlier studies [7]. Figure 9b shows the fraction of electromagnetic energy as a function of depth in the shower (in interaction lengths), which is obtained by integrating these components. The result is both surprising and (with hindsight) expected – a hadronic shower is almost entirely electromagnetic in nature in the first interaction length.

A small number of the features of hadronic showers remain to be described to complete the picture of the cascade. As discussed in [9], although the stochastic coefficient in the energy resolution of hadronic showers does scale with t_{had}, as expected, it has a non-zero intercept for t_{had}=0. This shows that the model including only sampling fluctuations is not

the full story and in fact indicates the importance of (nuclear) binding energy fluctuations to the response of the calorimeter.

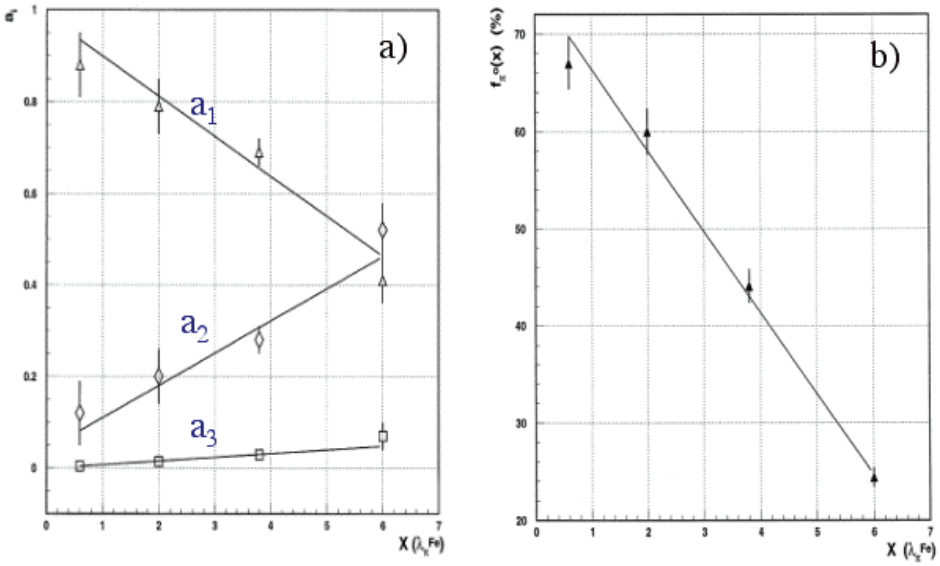

Figure 9, a) amplitude of the three components of the hadronic shower as a function of depth in interaction lengths, from fits as described in the text; b) fraction of electromagnetic energy in a hadronic shower as a function of depth in interaction lengths

As part of the "hanging file" calorimeter test at Fermilab for the SDC experiment [9], the evolution of hadronic showers was measured as a function of depth in a calorimeter with 96 sample layer in a total absorber of 6λ. The measurements showed significant fluctuations in the deposition of electromagnetic energy as a function of depth in the calorimeter as well as substantial event-to-event variation (depending primarily on the starting point of the electromagnetic cascade.) These fluctuations are local effects and any corrections to the response must be on an event-by-event basis. Hughes [10] also studied correlations between different sample layers in a hadron calorimeter. He found that early in the cascade, correlations were weak, whereas later in the shower strong sample-to-sample correlations exist. The understanding of such correlations is directly relevant to the corrections which must be applied to the observed response to correct for the effects of dead material (such as cryostats, coils and other absorber which is intrinsically not sampled by the active medium.)

5. SHOWER WEIGHTING BY POSITION (DEPTH) IN THE CALORIMETER

In Section 4, we were introduced to the many factors which complicate the simple picture of a hadronic shower as it develops and is measured in a calorimeter.

- The response to pions is not equal to that of photons and electrons
- The transverse shape of the shower reflects that of the energy deposition: narrow for electromagnetic, broad for non-electromagnetic
- A large fraction of the particle energy is ultimately deposited through electromagnetic showers

- Early in the hadronic cascade, the shower energy is deposited primarily electromagnetically
- Fluctuation in binding energy is intrinsic to hadronic cascades and appears to be the principal mechanism, which limits the precision with which the energy of the incident hadron may be measured.

Early in the development of the calorimeters for particle physics, shower energy weighting as a function of depth in the calorimeter was recognized as a means by which their energy resolution and linearity could be improved [11]. In these early studies the shower weights were determined experimentally for single pions and optimized to minimize the experimentally measured energy resolution of the calorimeter. At the LHC the calorimeter geometry is complex and in addition the energy scales extend well beyond those accessible to testbeams. As a result, Monte Carlo simulation of hadronic showers is used to determine weights and correction factors. Testbeam measurements still play a role, but in this case they are generally used to validate the assumptions used in the Monte Carlo simulation.

Although the focus of this lecture is hadron calorimetry, it is important to appreciate that even for the much simpler case of electromagnetic calorimetry, Monte Carlo weights may also be necessary to obtain the ultimate linearity and resolution of the detector. Such is the case for the ATLAS barrel liquid argon calorimeter where there is significant dead material in the tracking volume as well as between the different readout depths. The resulting cell energies are combined using the following formula, which has been optimized for both maximum linearity and minimum resolution.

$$E^{rec} = \left(a(E) + b(E)\ E_0^{vis} + c(E)\ (E_0^{vis} \cdot E_1^{vis})^{0.5} + \frac{1}{d(E)\ f_{samp}} \sum_{i=1,3} E_i^{vis} \right) \cdot f_{\text{cell impact}}(\Delta\Phi) \cdot (1 + f_{\text{leakage}})$$

The following terms illustrate the importance of the Monte Carlo simulation (in this case EGS4):

- The correction a(E) takes account of energy lost in the dead material upstream of the calorimeter.
- The term $(E_0.E_1)^{0.5}$ uses the correlation between the energy deposited in the two consecutive depth segments to correct for energy lost in dead material between them.
- f_{samp} can only be computed using the Monte Carlo and includes an implicit dependence of sampling fraction (i.e. detected ionization/deposited ionization) with depth in the shower.

GEANT4 [12] is now the most common Monte Carlo in use for full simulation of hadronic cascades and the determination of cell-weighting algorithms, directly analogous to that given above for electromagnetic showers, to optimize energy resolution and linearity. It is an ensemble of algorithms to model nuclear processes (such as fission, neutron evaporation, neutron transport, decays of unstable nuclei and fragmentation) as well as the EGS4 model for electromagnetic energy deposition (it is also an interesting anecdotal observation that nuclear physics in the region of 3-15GeV, as implemented in the Binary Cascade model or Bertini cascade model, plays a pivotal role in the transverse shower shape.)

The high energy models used for hadrons of energy between 15GeV and 10TeV are central to LHC shower simulation. There are in fact 3 models available in GEANT4:

- A parameterized high energy model depending on fits to experimental data with some theoretical guidance (HEP)
- A purely theoretical model with diffractive string excitation and decay to hadrons (QGS)
- An alternative theoretical model using Fritiof fragmentation (FTF)

The Monte Carlo calculations must be validated where possible. Where experimental data is available, these models are compared and tested, and in addition testbeam data for individual calorimeters are generally compared directly to the results of the Monte Carlo simulation. Of course this is not possible for the high energy models at the highest particle energies, and as a result it will be necessary to use in situ data to establish the systematic uncertainty on the energy scale at the highest energies to be recorded at the LHC. In fact an enormous amount of work has gone into the development and validation of the models and algorithms used in GEANT4. For further details on the GEANT4 package and the most recent results on its validation, the reader is referred to the presentations at the 2006 Calorimeter Conference [13] and references therein.

6. SINGLE PIONS TO JETS

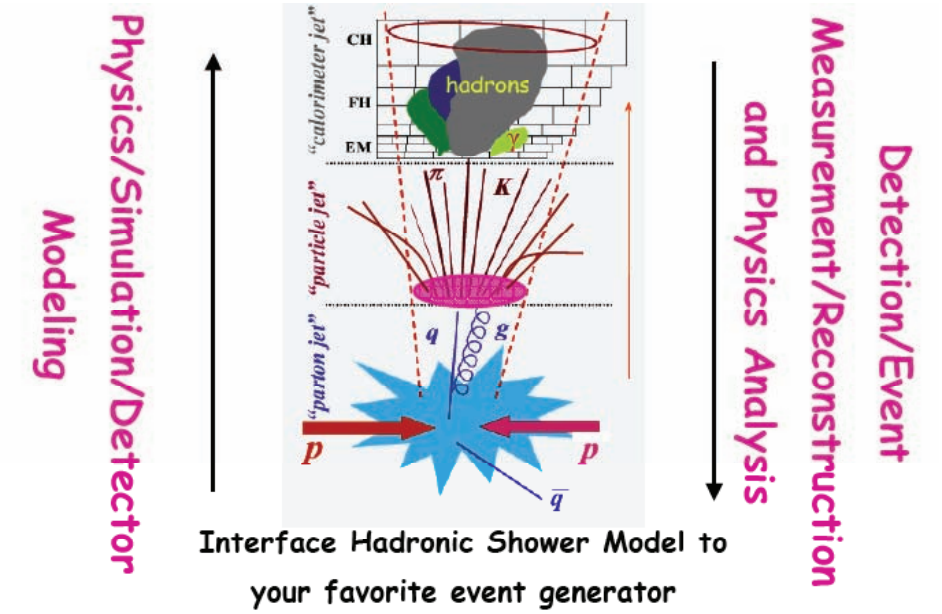

Figure 10, cartoon of the evolution from the partons produced in a hard scatter of two proton, through the QCD parton shower, particle jet and eventually to energy deposition in a combined calorimeter containing both an electromagnetic and hadronic section.

We have now reached the final topic in this discussion of hadron calorimetry, namely their use in jet energy reconstruction and measurement. Until now, we have discussed hadron calorimeters in the context of their response to

single particles. However, this is not the experimental situation – there we have jets. Figure 10 is a cartoon (whose originator is lost in the tendrils of the web) depicting the evolution of a jet resulting from a hard QCD scatter.

There are two points of note in Figure 10. The first is the naming convention in which the calorimeter is described as electromagnetic or hadronic. This simply reflects the fact that the first section of any calorimeter is typically higher performance, as it must measure electrons and photons from the primary interaction. Hadrons, of course interact here as well and these signals must be added to those in the hadronic calorimeter to recover the full pion (or jet) energy. The second is the fraction of jet energy, which is intrinsically electromagnetic (principally photons from π^0's produced in the hard scatter.) This is approximately 25% of the total jet energy, as is shown in figure 11, which is the result of a Pythia simulation [14].

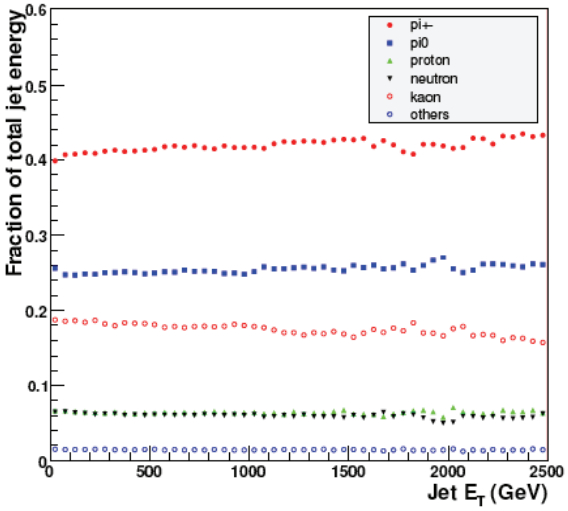

Figure 11, Pythia simulation giving the energy fraction carried by different stable particle species as a function of jet energy

In going from single pions to jets, we therefore have to accommodate many different characteristics of the calorimeter as a whole. Photons and electrons from the primary interaction deposit their energy in the "electromagnetic" section, where we also have some probabilistic energy deposition by charged and neutral hadrons. Deeper in the calorimeter the energy comes primarily from the charged and neutral hadrons, but may be electromagnetic in nature as a result of interactions in the absorber which produce π^0s. In addition, the intrinsic response is general different for electromagnetic and non-electromagnetic energy deposition ($e/h \neq 1$).

The means by which the jet energy is reconstructed follows directly by analogy to the weighting scheme described above for single pions. We determine cell and/or layer weights, which account for jet fragmentation (i.e. characterized by the particle species and energy distribution) as well as the shower development characteristics of single particles. Unlike the case for single particles, these weights must be determined using Monte Carlo simulation. The specifics of these weighting schemes depend on the detailed geometry and properties of the calorimeter in question, and I will address them in the context of the ATLAS calorimeter (CMS has performed similar studies.)

A simplified layout of the central barrel calorimeter geometry of ATLAS is shown in Figure 12. As can be seen in this cartoon, the electromagnetic section of the calorimeter has both three readouts in depth and fine cell granularity. The hadronic section also three readouts, whose depth segmentation was optimized on energy resolution using data obtained in a prototype calorimeter module. Three general types of algorithm are being developed by ATLAS to optimize jet energy linearity and resolution:

1. The first uses cell energy density to characterize energy deposition as either electromagnetic or hadronic in nature. High energy density is a feature of electromagnetic showers whose transverse and longitudinal shower size is characterized by the Moliere radius. Hadronic energy is characterized by the hadronic interaction length and hence has lower energy density. The electromagnetic energy is included in the energy sum with a unit weight (as this is the basic calibration), while the hadronic energy is weighted when it is included in the energy sum. The weights are determined by optimization of the energy resolution using Monte Carlo simulation of QCD jets. In this method the weights are independent of jet energy. This approach is similar to that used by H1 [15]

2. The second method is identical to the first with the difference that the weights are allowed to depend on the jet energy. Clearly in this case an iterative procedure is needed, since the jet energy is not known *a priori*.

3. The third approach (and the one, whose development I contribute to) is based entirely on weighting cells by depth (layer) in the calorimeter. One might initially believe that this is too simple. However, as was shown above, the early part of the shower from a hadronic interaction is primarily electromagnetic in nature. Therefore, this component of the shower energy is wholly independent of particle species and one can simply add the energy deposition from primary photons and electrons to that from hadrons and treat it entirely as electromagnetic in nature. Beyond $24X_0$, all energy from primary photons and electrons has been absorbed and what remains is energy deposition from the primary hadrons. In the early part of the hadronic calorimeter, this is both electromagnetic and hadronic in nature, while at the back of the calorimeter, as indicated in Figure 12, it is essentially entirely hadronic in nature. The weights are again optimized using a Monte Carlo simulation of QCD jets, and are energy dependent (therefore an iterative procedure is used.) One final note is that it is important to recognize that these weights may also be dependent on jet fragmentation, which can be characterized by the energy fraction in the electromagnetic section.

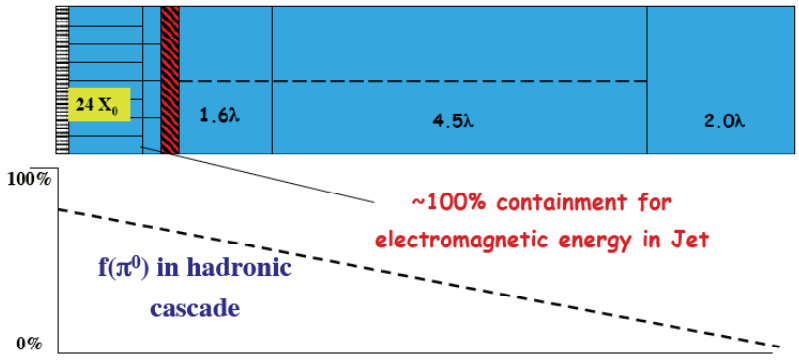

Figure 12, schematic layout of the central barrel calorimeter in ATLAS showing the shower containment in interaction lengths, l, as well as indicating the granularity of the readout cells. The line $f(\pi^0)$ indicates the electromagnetic fraction of the hadronic cascade as a function of shower depth [8].

All three methods must include a treatment for noise in the calorimeter as well as corrections for dead material between sampling layers (such as is shown above for the measurement of electrons in the ATLAS liquid argon barrel calorimeter.) The weights are determined by the optimization of the resolution and linearity of the reconstructed jet energy against Monte Carlo "truth", in the corresponding jet cone – equivalent to the "particle jet" in Figure 10 above.

As one of the proponents of approach 3, and since I like its simplicity and elegant interpretation on the intrinsic properties of the hadronic cascade, I will show the result from it. Figure 13 shows the energy resolution at the basic calibration scale of the ATLAS calorimeter (the electromagnetic scale) and for the sample-weighted calibration (method 3.) [16] The improvement in jet energy resolution and linearity is dramatic, and clearly demonstrates the validity of the underlying premise in this method. It is, however, important to note that all three methods give good performance, with method 2 perhaps providing the best resolution. Eventually, the differentiating characteristic between these methods may come from the systematic uncertainties associated with each of them, and which are presently under study.

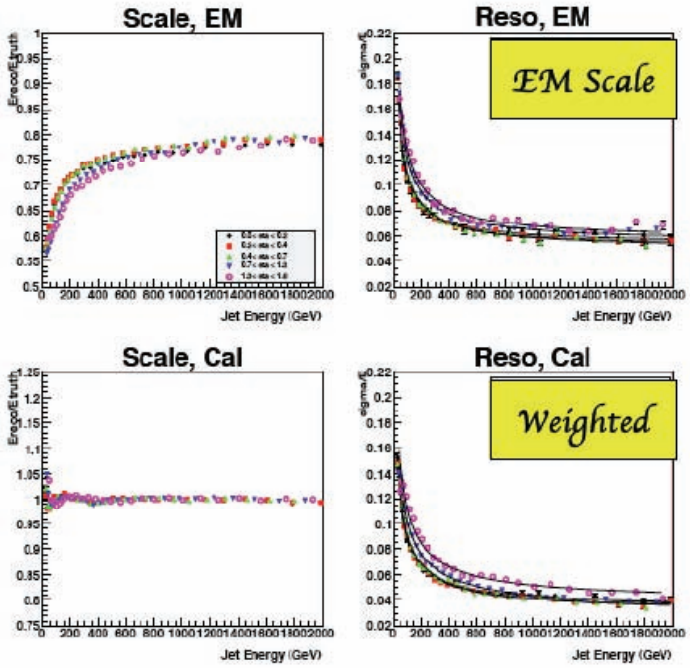

Figure 13, preliminary results from jet weighting method 3 [16], as described in the text. The different points represent different regions of detector pseudo-rapidity.

7. SUMMARY

In this lecture I have taken you from the basic physics requirements of hadronic calorimeters, through some details of their construction and performance to the physics of hadronic showers and eventually to jet energy measurement. I hope that I have convinced you that the reconstruction of jet energies is one of the more complex analysis procedures of any at the LHC, and that precision reconstruction of jets is not possible without a segmented calorimeter and detailed, tuned Monte Carlo codes describing the interactions of particles with matter. Hadron calorimeters may indeed be "blunt

objects", as my friend and colleague Dan Green has often stated, but without them many of the physics processes at the LHC will be lost to our study. Indeed, SUSY will be first signaled by high P_t jets and missing transverse energy reconstructed with precision in these detectors.

Acknowledgements

I would like to thank the organizers, and in particular Joanne Hewitt, for their hospitality and invitation to present a lecture at the SLAC Summer Institute. I particularly enjoyed attending many of the lectures - as a member of the ATLAS collaboration who spent much of the last 10 years building a section of calorimeter, they provided a timely reminder of the enormous wealth of physics we are about to uncover when the LHC turns on. The beach barbeque with my new ATLAS colleagues from the SLAC Group, was an unexpected experience and one of the highlights of the two weeks. Finally, in preparing this lecture, I have called upon over 20 years of designing, constructing, and using calorimeters for physics analysis as a member of the CDF, SDC and ATLAS collaborations. Along the way I have had the privilege of working with some talented and inspired individuals and would like to thank in particular Barry Wicklund, Panakanal Job, Dan Green and Ambreesh Gupta for their contributions to my own understanding of calorimetry.

Work supported in part by the U. S. Department of Energy, Division of High Energy Physics, contract number W-31-109-ENG-38.

References

[1] At the time of the written version of this lecture, the top mass measured by the combination of data from D0 and CDF is 171.4GeV, to which the contribution from the jet energy scale systematic uncertainty is 1GeV (hep-ex/0608032.)
[2] Euro Phys J C 39:s63-s90 (2005)
[3] The ATLAS Detector**,** http://atlas.web.cern.ch/Atlas/index.html
The CMS Detector, http://cms.cern.ch/
[4] Particle Data Group, http://pdg.lbl.gov/2006/reviews/pardetrpp.pdf, M. Kobyashi, http://kaon.kek.jp/~scintikek/pdf/koen-17-nov.pdf
[5] Amaldi, Physica Scripta Vol 23:409-424 (1981)
[6] Gabriel et al. NIM A927:1-99 (1993)
[7] Friend et al. NIM 136 :505-510 (1976)
[8] Amaral et al. NIM A443 :51-70 (2000)
[9] Beretvas et al. NIM A329:50-61 (1993)
Green, Fermilab Academic Lecture, http://www-ppd.fnal.gov/eppofficew/Academic_Lectures/Past_Lectures.htm
[10] Hughes, SLAC-PUB 404 (1990)
[11] Abramowicz et al. NIM 180:429-439 (1981)
[12] GEANT4, http://geant4.web.cern.ch/geant4/
[13] CALOR06, http://calor.pg.infn.it/calor2006.htm
[14] A. Gupta, private communication.
[15] H.-P. Wellisch et al. Hadronic Calibration of the H1 LAr Calorimeter using Software Weighting Techniques, MPI Report MPI-PhE/94-03 (1994)
C. Issever et al. http://arxiv.org/pdf/physics/0408129
[16] A. Gupta, F. Merritt and J. Proudfoot, ATLAS simulation (preliminary analysis)